

## Effects of Corner Geometry and Adiabatic Extensions on Heat Transfer through a Differentially Heated Square Cavity

C. Lei<sup>1</sup>, S.W. Armfield<sup>2</sup>, J.C. Patterson<sup>1</sup> and A. O'Neill<sup>1\*</sup>

<sup>1</sup>School of Engineering  
 James Cook University, Townsville, QLD 4811 AUSTRALIA

<sup>2</sup>School of Aerospace, Mechanical and Mechatronic Engineering  
 The University of Sydney, Sydney, NSW 2006, AUSTRALIA

\*Current address: Reliability Engineering  
 Rio Tinto Aluminium – Yarwun, Gladstone DC, QLD 4680, AUSTRALIA

### Abstract

This study is concerned with heat transfer by natural convection in a differentially heated square cavity. The purpose is to explore numerically the effects of the corner geometry and adiabatic extensions on heat transfer through the sidewalls. Two sets of simulations have been carried out in this study. The first set is concerned with steady-state calculations with different corner shapes, and the second set considers both steady-state and transient heat transfer with adiabatic extensions of various dimensions. The numerical results are presented in this paper.

### Introduction

A differentially heated cavity is an appropriate model for many engineering applications. Typical examples include heat exchangers and cooling of electronic devices. Currently many electronic cooling systems still rely on forced convection that requires the use of external devices such as fans or pumps (hereinafter referred to as active cooling systems). Active cooling systems present several problems such as reliability, noise and additional power consumption. Compared to active cooling systems, passive cooling systems by pure natural convection do not require external devices and have several advantages such as high reliability and low noise. However, passive cooling systems, in general, cannot achieve a rate of cooling that is comparable with that of active cooling systems. Therefore, studies on the enhancement of heat transfer by natural convection have been very active in recent years [1-4].

In this study, the effect of the corner geometry and adiabatic extensions on heat transfer by natural convection through a differentially heated square cavity is investigated numerically. The base model is a two-dimensional (2D) rectangular cavity of a height  $H$  and a width  $L$ , resulting in an aspect ratio (height-to-width ratio)  $A = H/L$ . The cavity contains water as the medium with an initial temperature of  $T_0$  and an initial velocity of zero everywhere. The two sidewalls of the cavity are heated to  $T_H = T_0 + \Delta T$  and cooled to  $T_C = T_0 - \Delta T$  respectively, where  $\Delta T$  is the absolute temperature difference between the sidewalls and the mean interior temperature. The top and bottom boundaries are adiabatic. Two sets of simulations have been carried out in this study. First, steady-state calculations are conducted with different corner shapes including sharp, round and straight corners, all of which are assumed adiabatic. The numerical results are compared with the base model. In the second set of simulations, both steady-state and transient calculations are conducted with adiabatic extensions of various dimensions. Details of the numerical procedures and results are presented in the following sections.

### Governing Equations and Numerical Methods

In this study, the aspect ratio of the base model is fixed at  $A = 1$  (*i.e.* a square cavity). With water as the medium in the cavity, heat transfer by natural convection through the base model of a differentially heated cavity is characterized by the Grashof number ( $Gr$ ) or Rayleigh number ( $Ra$ ), which are defined as:

$$Gr = \frac{g\beta\Delta TH^3}{\nu^2} \quad (1)$$

$$Ra = Pr \cdot Gr \quad (2)$$

where  $g$  is the acceleration due to gravity,  $\beta$ ,  $\nu$  and  $Pr$  are the coefficient of thermal expansion, kinematic viscosity, and Prandtl number of water, respectively. All the fluid properties are evaluated at the mean water temperature  $T_0$ .

The temperature and flow structures within the cavity, which is determined by a natural convection process, can be described by the following set of governing equations, for which the Boussinesq assumption has been made:

$$\frac{\partial u}{\partial x} + \frac{\partial v}{\partial y} = 0 \quad (3)$$

$$\frac{\partial u}{\partial t} + u \frac{\partial u}{\partial x} + v \frac{\partial u}{\partial y} = -\frac{1}{\rho} \frac{\partial p}{\partial x} + \nu \nabla^2 u \quad (4)$$

$$\frac{\partial v}{\partial t} + u \frac{\partial v}{\partial x} + v \frac{\partial v}{\partial y} = -\frac{1}{\rho} \frac{\partial p}{\partial y} + \nu \nabla^2 v + g\beta(T - T_0) \quad (5)$$

$$u \frac{\partial T}{\partial x} + v \frac{\partial T}{\partial y} = \kappa \left( \frac{\partial^2 T}{\partial x^2} + \frac{\partial^2 T}{\partial y^2} \right) \quad (6)$$

where  $u$  and  $v$  are the velocity components in the  $x$  and  $y$  directions respectively;  $T$  is the water temperature;  $p$  is the pressure; and  $\rho$  and  $\kappa$  are the density and thermal diffusivity of water respectively evaluated at the reference temperature  $T_0$ .

The above governing equations along with the specified boundary and initial (for transient calculations only) conditions are solved using a Finite Volume Method. The SIMPLE scheme is adopted for pressure-velocity coupling; and the spatial discretization is done by a second-order upwind scheme. For the transient flow calculations, time marching is by a second-order implicit scheme.

Non-uniform meshes are constructed for all models in this study. A mesh dependence test is conducted using the base model (*i.e.* a square cavity with the sidewalls either heated or cooled). The test is carried out for two Rayleigh numbers of  $Ra = 2.22 \times 10^8$  and  $1.1 \times 10^9$  respectively. Two meshes with a total number of approximately 16,000 and 50,200 cells respectively are

constructed. The numerical results are compared in table 1 below, which shows the calculated Nusselt numbers using the two different meshes and for the two different Rayleigh numbers.

Mesh	$Ra = 2.22 \times 10^8$	$Ra = 1.11 \times 10^9$
Mesh 1 (16,000 cells)	93.72	142.19
Mesh 2 (50,200 cells)	93.74	142.23
Variation	0.02%	0.03%

Table 1. Calculated Nusselt numbers with different meshes.

It is seen in table 1 that refining the mesh from 16,000 cells to 50,200 cells has a negligible effect on the calculated heat transfer for both Rayleigh numbers. Therefore, the coarse mesh is adopted for all the calculations with the base model in this study. For models with either modified corner geometry or adiabatic extensions (refer to the next section), the mesh is constructed in accordance with the mesh required for the base model. It is expected that the modification of the corner geometry and the addition of adiabatic extensions would not affect the flow significantly. Therefore, no separate mesh dependence tests are conducted for other models.

For the unsteady calculations, the time step is normally determined based on a time-step dependence test. A meaningful time-step dependence test for the present study would involve calculations of the flow from the initial start-up through to the final steady state with different time steps. However, these calculations are extremely expensive from the computational resource point of view, and are not feasible with the current computing resources. In this study, the time step is selected with reference to the time steps adopted in [5, 6], which determined the time step based on tests of the start-up flow only. Since the Rayleigh number considered in this study is lower than those considered in [5, 6], it is expected that an equivalent or smaller time step compared with those adopted in [5, 6] would provide sufficient accuracy for unsteady calculations.

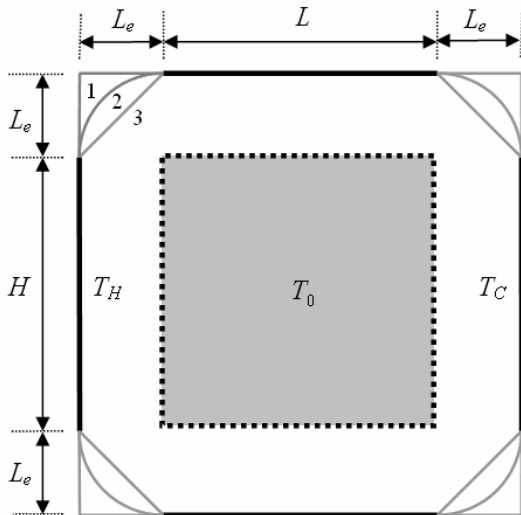


Figure 1: Extended square cavity with different corner shapes.

## Numerical Procedures and Results

### Effect of Different Corner Shapes

In order to examine the effect of corner geometry on heat transfer through the differentially heated cavity, the base model of the square cavity is extended equally in all directions (left, right, top and bottom) by a length of  $L_e$ , and corners of different shapes including sharp (1), round (2) and straight (3) corners respectively are added (see figure 1). The shaded region enclosed by dotted lines in figure 1 represents the original base model. All

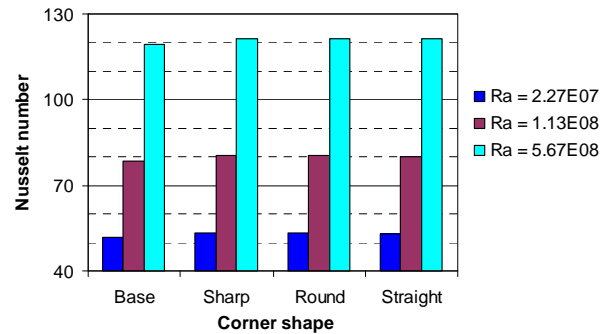
the added corners are assumed adiabatic, and thus, the lengths over which heat is transferred to and from the cavity remain unchanged, resulting in the same Rayleigh number for different corner shapes.

We introduce a new dimensionless parameter, the adiabatic extension ratio  $A_e$ , to quantify the geometric change. The adiabatic extension ratio is defined as:

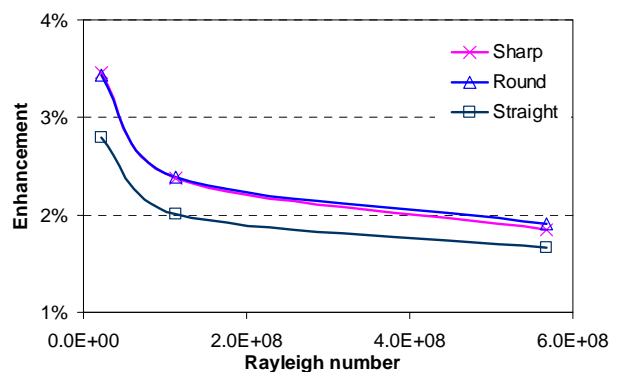
$$A_e = \frac{L_e}{H} \quad (7)$$

For the investigation of the effect of different corner shapes, the adiabatic extension ratio is fixed at  $A_e = 0.125$ . Steady-state calculations are conducted for three moderate Rayleigh numbers of  $Ra = 2.27 \times 10^7$ ,  $1.13 \times 10^8$  and  $5.67 \times 10^8$  respectively with a fixed Prandtl number of 6.62. The numerical results are presented in figure 2.

Figure 2(a) shows the calculated steady-state Nusselt numbers on the heated sidewall with different corner geometries. It is clear that, with all the geometric configurations including the base model, the calculated Nusselt number increases with the Rayleigh number. It is also noticeable that there is a slight increase in the steady-state Nusselt number with the modified corner geometries (*i.e.* with sharp, round or straight adiabatic corners) compared with the base model, suggesting that the steady-state heat transfer through the hot sidewall is enhanced.



(a) Calculated Nusselt numbers with different corner shapes and for different Rayleigh numbers



(b) Enhancement of heat transfer for different Rayleigh numbers obtained with different corner shapes

Figure 2: Steady-state Nusselt number and enhancement of heat transfer on the hot wall with different corner geometries and for different Rayleigh numbers.

The extent of heat transfer enhancement due to the modifications to the corner geometry is shown in figure 2(b) for different Rayleigh numbers. Clearly, for all the three shapes of the corner geometry, the enhancement of heat transfer increases with decreasing Rayleigh number, and a better enhancement is achieved with either sharp or round corners. For the lowest Rayleigh number considered here (*i.e.*  $Ra = 2.27 \times 10^7$ ), the

maximum enhancement is 3.5% with sharp corners, and the enhancement reduces to 2.8% with straight corners.

Both sharp and round adiabatic corners have similar effect on the calculated Nusselt number on the hot wall, and they result in a better enhancement of heat transfer compared with the straight corners. Hence, in the following section, the effect of the adiabatic extension ratio on heat transfer is examined based on sharp corners only due to their relatively simplicity for mesh generation.

**Effect of Adiabatic Extensions**

In this section, the effect of adiabatic extensions of various dimensions on heat transfer through the sidewalls is investigated. For this purpose, the sidewalls are extended vertically in two opposing directions while the width of the differentially heated cavity remains unchanged (see figure 3). Similarly, the extended sections of the sidewalls are assumed adiabatic, and thus the Rayleigh number remains the same. Both steady-state and transient features of heat transfer with the adiabatic extensions are considered.

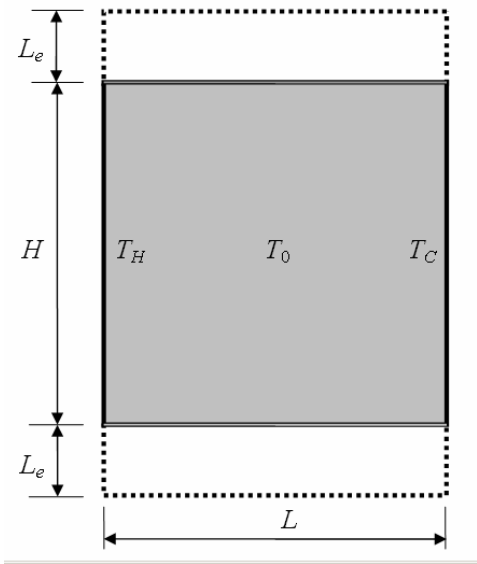


Figure 3: Differentially heated cavity with adiabatic extensions.

First, a series of steady-state calculations are carried out for adiabatic extension ratios ranging from  $A_e = 0.01$  to 0.3. The Rayleigh number is fixed at  $Ra = 2.22 \times 10^8$  and the Prandtl number is fixed at  $Pr = 6.62$ . The calculated Nusselt numbers on the hot wall for different adiabatic extension ratios are presented in figure 4.

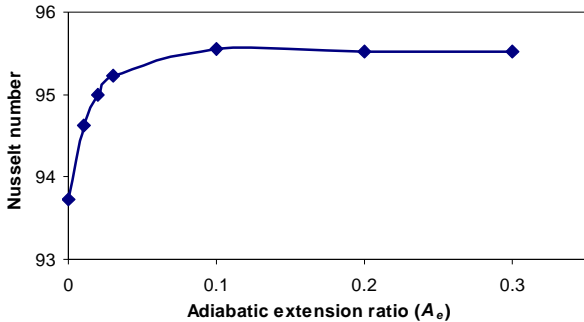
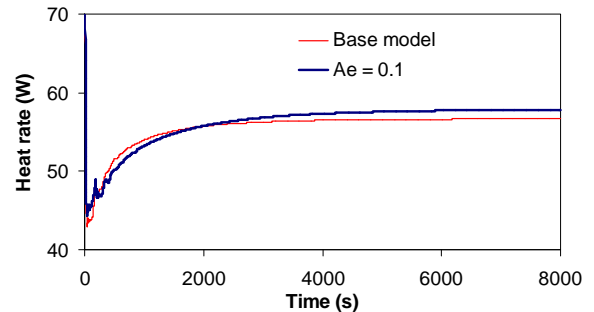


Figure 4: Calculated steady-state Nusselt number on the hot wall for various adiabatic extension ratios.

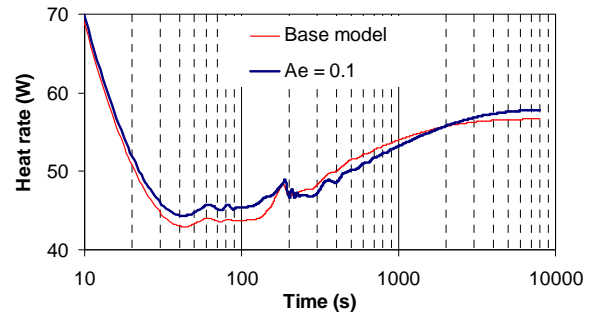
It is clear in figure 4 that, as the adiabatic extension ratio increases from zero, the calculated Nusselt number initially

increases, indicating that heat transfer through the sidewall is enhanced with the addition of the adiabatic extension. However, as the adiabatic extension ratio is increased beyond 0.1, there is no further increase of the calculated Nusselt number. The maximum enhancement of the steady-state heat transfer is about 1.9% for the current Rayleigh number.

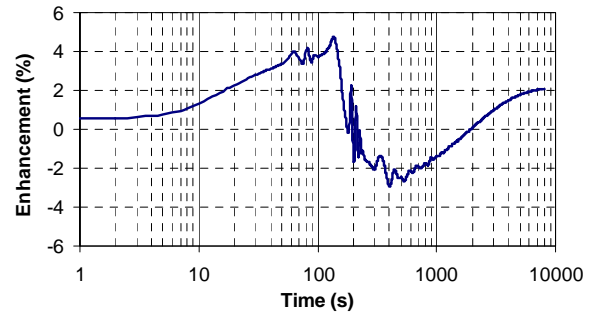
Next, the effect of the adiabatic extension on transient heat transfer is investigated for a fixed adiabatic extension ratio of  $A_e = 0.1$  and for the same Rayleigh and Prandtl numbers as the steady-state calculations. The parameters are selected based on a physical model with a height of 0.24 m. The reference temperature is set at 295 K, and the temperature difference is fixed at  $\Delta T = 1$  K, resulting in a Rayleigh number of  $Ra = 2.22 \times 10^8$ . A dimensional time step of 0.1 s is adopted for the unsteady calculations. The model is calculated with and without the adiabatic extensions for comparison purposes. The numerical results are shown in figure 5.



(a) Time history of the heat rate on the hot sidewall plotted in a linear time scale.



(b) Time history of the heat rate on the hot sidewall plotted in a logarithmic time scale.



(c) Time history of the enhancement of heat transfer.

Figure 5: Effect of the adiabatic extension on transient heat transfer through the hot sidewall.

Plotted in figure 5(a) are the time histories of the calculated heat transfer rate through the hot sidewall in a linear time scale. It is seen in figure 5(a) that, for both cases with and without the adiabatic extensions, the calculated heat transfer rate undergoes a transition and gradually approaches a constant at the steady state.

In order to clearly demonstrate the heat transfer features at the early start-up and transitional stages, the calculated heat transfer rate through the hot sidewall is replotted in a logarithmic time scale in figure 5(b). Clearly, the major features of the flow in the early and transitional stages are the same with and without the adiabatic extensions. In the early stage, the calculated heat transfer rate with the addition of the adiabatic extensions surpasses that obtained with the base model. The comparison of the heat transfer rate is reversed after about 200 s, which approximately corresponds to the time when the intrusion flows arrive at the opposing sidewalls. This remains to be the case until around 1900 s when the heat transfer rate calculated with the adiabatic extensions again surpasses that without the extensions. It is noticed that the second switch of the comparison between these two models occurs after the perturbations induced by the arrival of the intrusion flow from the cold wall die out.

Figure 5(c) shows quantitative information of the enhancement of transient heat transfer due to the addition of the adiabatic extensions. It confirms that heat transfer through the hot wall is enhanced from the start-up until the arrival of the intrusion from the cold wall (around 200 s). A maximum heat transfer enhancement of 4.75% is observed at 137 s after the start-up. Associated with the flow oscillations induced by the arriving intrusion (during the period from approximately 200 to 1900 s), heat transfer through the hot wall is depressed due to the presence of the adiabatic extensions. After the flow oscillations die out, heat transfer is again enhanced with the adiabatic extensions. This remains to be the case for the rest of the flow transition until the final steady state, at which heat transfer is enhanced by about 2.1%.

Note that the enhancement of the steady-state heat transfer calculated using the unsteady model (2.1%) is slightly higher than that predicted by the steady model (1.9%). This may be attributed to two factors. Firstly, the final state of the unsteady model (*i.e.* at 8000 s) is not at a truly steady state since the transition to the steady state is an extremely slow process. To cover the complete transition to the final steady state would require significant computing resources, and is not feasible. Therefore, the present calculation is terminated at 8000 s. Secondly, for unsteady calculations, an additional numerical error associated with the finite time step is inevitable.

It can be estimated from figure 5(c) that the overall effect of adding the adiabatic extensions is a net 1% enhancement of heat transfer through the hot wall for the period covered by the calculation. It is also expected that the net effect of the adiabatic extensions on transient heat transfer depends on both the Rayleigh number and the adiabatic extension ratio.

## Summary

It is not uncommon to speculate that heat transfer through a differentially heated cavity is controlled by the length of the sidewall over which the cavity is heated and cooled. The heating and cooling length of the sidewalls also determines the Rayleigh number of this problem, which, along with the Prandtl number

and aspect ratio, governs natural convection in the cavity. However, the present study has demonstrated that heat transfer through the cavity can be enhanced by modifying the geometry while keeping the heating and cooling lengths of the sidewalls unchanged.

It is revealed in this study that adding adiabatic extensions to the differentially heated cavity enhances steady state heat transfer to a certain extent (refer to figure 4). Further extending the domain provides no additional benefit in terms of heat transfer. The enhancement of heat transfer due to the adiabatic extensions depends strongly on the Rayleigh number (refer to figure 2b). The lower the Rayleigh number, the better enhancement is achievable. It is also found in this study that the geometry of the corners on an extended domain has minor effect on heat transfer (figure 2). However, a slightly reduced enhancement of heat transfer is obtained with the straight corners compared to sharp and round corners.

The numerical results based on an unsteady model further demonstrate that better enhancement of heat transfer can be achieved at the early stage of the flow development following the start-up (refer to figure 5c). However, heat transfer is depressed during the early transitional stage following the arrival of the intrusion from the opposing sidewall. During the late transition toward the final steady state, the addition of the adiabatic extensions again enhances heat transfer. It is worth investigating the enhancement of transient heat transfer with different adiabatic extension ratios and for different Rayleigh numbers in future.

## Acknowledgement

The authors are grateful for the financial support of the Australian Research Council.

## References

- [1] Costa, V.A.F., Oliveira, M.S.A. & Sousa, A.C.M., Control of laminar natural convection in differentially heated square enclosures using solid inserts at the corners, *International Journal of Heat and Mass Transfer*, **46**, 2003, 3529-3537.
- [2] Ichimiya, K., Heat transfer enhancement or depression of natural convection by a single square solid element on or separated from a vertical heated plate, *Enhanced Heat Transfer*, **7**, 2000, 125-138.
- [3] Tasnim, S.H. & Collins M.R., Numerical Analysis of Heat Transfer in a Square Cavity with a Baffle on the Hot Wall, *International Communications in Heat and Mass Transfer*, **31**, 2004, 639-650.
- [4] Xu, F., Patterson, J.C. & Lei, C., Experimental observations of the thermal flow around a square obstruction on a vertical wall in a side-heated cavity, *Experiments in Fluids*, **40**, 2006, 364-371.
- [5] Patterson, J.C. & Armfield, S.W., Transient Features of Natural Convection in a Cavity, *Journal of Fluid Mechanics*, **219**, 1990, 469-497.
- [6] Xu, F., Patterson, J.C. & Lei, C., (2004) Oscillations of the horizontal intrusion in a side-heated cavity, in *Proceedings of the Fifteenth Australasian Fluid Mechanics Conference (CD-ROM)*, editors M. Behnia, W. Lin and G.D. McBain, The University of Sydney, 2004, Paper AFMC00243.